

Utilization of Departmental Computing GRID System for Development of an Artificial Intelligent Tapping Inspection Method, Tapping Sound Analysis

Seung Jo Kim[†], Joon-Seok Hwang* and Chang Sung Lee*

Department of Aerospace Engineering, Seoul National University, Korea

Sangsan Lee*

High Performance Computing and Networking Supercomputing Center, KISTI, Korea

Abstract

Tapping Sound Analysis is a new NDE method, which determines the existence of subsurface defects by comparing the tapping sound of test structure and original healthy structure. The tapping sound of original healthy structure is named sound print of the structure and is obtained through high precision computation. Because many tapping points are required to obtain the exact sound print data, many times of tapping sound simulation are required. The simulation of tapping sound requires complicated numerical procedures. Departmental Computing GRID system was utilized to run numerical simulations. Three cluster systems and one PC-farm system comprise DCG system. Tapping sound simulations were launched and monitored through *Globus* and *CONDOR*. A total of 160 Tera floating-point (double-precision) operations was performed and the elapsed time was 41,880 sec. From the numerical experiments, Grid computing technology reduced the necessary time to make sound print database and made TSA a feasible and practical methodology.

0-7695-1524-X/02 \$17.00 (c) 2002 IEEE

[†] Professor, San 56-1, Shilliom-dong Kwanak-gue, Seoul, 151-742, Korea, E-mail: sjkim@snu.ac.kr

♣ Graduated Student,

* Director, Korean Institute of Science and Technology Information, Taejon 305-333, Korea

1. Introduction

In aerospace application, composite materials have been extensively used due to their good material properties. Laminated composites, which are general forms of composite structure, are made in the shape of plate or shell and the thickness is relatively smaller than other dimensions. Therefore, laminated composites are weak under transverse loading condition. For example, low speed impact causes delamination in the laminated composites. In addition, if there is imperfection of curing caused by the mistakes in manufacturing process, structural safety is not guaranteed. Because these defects are hardly detected by naked eyes, some systematic inspection methods are needed. To detect the defects inside the structures, nondestructive evaluation (NDE) is widely used for the inspection systems. However, these methods are cumbersome and sometimes expensive.

On the other hand, by hearing the tapping sound radiated from the test structures, experienced inspectors can detect defects. The tapping sound from the defective structure is different from that of healthy one, so the existence of defects can be known by the subtle difference of the tapping sound. Although simple and convenient, this method is not founded systematically and totally depends on the experiences of inspectors. With this background, we are developing a new NDE method, which utilizes the tapping sound of structure to determine existence of defects inside the structure. This new NDE method as an AI (Artificial Intelligent) tapping inspection method is named *Tapping Sound Analysis (TSA)* [1].

If subsurface defects have formed in the structure during the manufacturing or operation time, the structural properties will be altered. The alteration of structural properties due to the subsurface defect results in slight changes in the tapping behavior of the structure. At first, the contact force profile will change. And the tapping sound also will be changed due to the existence of subsurface defects. Tapping sound analysis uses these slight changes in the tapping sound as the criterion to determine the existence of subsurface defect. To find the changes in the tapping sound, the tapping sound of test structure is compared with that of the original healthy structure. Tapping sound data of the original healthy structure is used as a reference data and named *sound print* of the structure. The sound print is a unique property of the structure, like a human fingerprint.

As a reference data, the sound print should be objective and absolute because the performance of tapping sound analysis depends on the sound print. An easy way to obtain sound print may be obtaining by repeated measuring of the tapping sound of the real healthy structure. The test data of healthy structure is recorded *a priori* and accumulated as the sound print database. However, if perfection of real healthy structure is not guaranteed, the objectivity of the sound print measurement is also not guaranteed. As a more objective way, the sound print can be obtained by high precision computations. For the precise calculation of the tapping sound data, a detailed modeling of the tapping event and the sound radiation should be needed. In some sense,

numerical simulations based on a detailed modeling give more objective sound print than real measurements do. Moreover, during the design stage of the structure the sound print can be obtained and accumulated as the database.

In order to form sound print database, tapping sound data of many tapping points should be computed. Simulation of tapping sound data requires very complicated numerical procedures. And as the test surface becomes wider, at least hundreds of tapping points should be needed. Therefore, huge amount of numerical computation is required to form the sound print database and it may take several months to obtain satisfactory sound print database of structures on a single machine. Moreover all numerical simulations must be re-run if a measuring point will be changed. Under this situation, it is not feasible to apply TSA for real structures health monitoring. In this case, Grid [2] computing technology may be a good solution to obtain required computing power. Basically, Grid computing technology was introduced to make huge applications, which require vast computing power beyond that available at any site, be executed by assembling systematically the geographically distributed supercomputers. However, Grid computing technology provides also an economical alternative to researchers. The computing power and resources of distributed PCs can be utilized for research and development through Grid computing technology. Hundreds or thousands of computers may be sitting idle at any major university in the dead of night. Several research projects, such as *Globus*[3], *Legion*[4], and *CONDOR*[5] are developing software infrastructures for building Grid computing system by using these idling systems. As well-known, *Globus* is a toolkit for Grid computing and provides various functional utilities for building computing Grid system, such as user authentication, information services, data management, etc and *CONDOR* converts collections of distributed PCs and cluster system into a distributed high-throughput computing facility. In this work, DCG (Departmental Computing Grid) system was built through *Globus* and *CONDOR* and utilized for tapping sound simulations. Distributed computing resources maintained and used by laboratories in department of aerospace engineering, Seoul National University were converted into *CONDOR* pools and users certificated through *Globus* can submit their jobs to *CONDOR* pools. The sound print database of structures can be obtained fast by using DCG system and no additional cost is required to run hundreds of tapping sound simulation jobs. This reduction in the time necessary to run tapping sound simulations makes TSA a feasible methodology.

2. Numerical Modeling of Tapping Sound

As an objective way to obtain sound print of a structure, numerical simulation of tapping sound consists of three parts: simulation of tapping event, simulation of vibration of structure due to the tapping force and calculation of the tapping sound radiated from the surface of structure.

The tapping event can be modeled as impact on the laminated composites by a tapping object. In general, impact problem is very difficult to solve because the load is transferred by the contact between impacting object and structures. Several numerical models were proposed for the simulation of impact phenomenon. Because we are treating the laminated composite structure, impact problems should be treated by dynamic contact algorithm considering both the impacting object and laminated composites for the precise calculation of contact force [6]. The vibrating motion of structure is calculated using finite element method. Space-discretized equation of motion is integrated using time integration method. The contact force is combined in the equation of motion. For the time integration method, central difference method is adopted in this work. The tapping sound can be modeled as the radiated sound from vibrating structure. Boundary element method can be successfully utilized for the simulation of tapping sound.

3. Numerical Modeling of Tapping Event

The matrix form of the space-discretized equation of motion [7] can be obtained as

$$\mathbf{m}\mathbf{a} + \mathbf{k}\mathbf{u} = \mathbf{f} \quad (1)$$

where \mathbf{m} is mass matrix, \mathbf{k} is the stiffness matrix, \mathbf{f} is external force and \mathbf{a} , \mathbf{u} are acceleration vector and displacement vector, respectively. The acceleration and displacement are space-discretized and functions of time. The time history of acceleration and displacement can be obtained through time integration. The central difference method [7] is used as the time integration method in this paper. The central difference method is a representative explicit time integration method. The central difference method uses two assumptions for the time derivatives. The assumptions for the time derivatives are as follows:

$$\mathbf{a}_n = \frac{1}{\Delta t^2} (\mathbf{u}_{n+1} - 2\mathbf{u}_n + \mathbf{u}_{n-1}) \quad (2)$$

$$\mathbf{v}_n = \frac{1}{2\Delta t} (\mathbf{u}_{n+1} - \mathbf{u}_{n-1}) \quad (3)$$

where $(n-1)$, n and $(n+1)$ denote the times of $(t_n - \Delta t)$, t_n and $(t_n + \Delta t)$, respectively. To construct a time integration algorithm, the dynamic equilibrium equation at time t is considered.

$$\mathbf{m}\mathbf{a}_n + \mathbf{k}\mathbf{u}_n = \mathbf{f}_n \quad (4)$$

Substituting the relations for \mathbf{a} and \mathbf{v} in Eq. (2) and Eq. (3) into equation (4), we obtain

$$\left(\frac{1}{\Delta t^2} \mathbf{m} \right) \mathbf{u}_{n+1} = \mathbf{f}_n - \left(\mathbf{k} - \frac{2}{\Delta t^2} \mathbf{m} \right) \mathbf{u}_n + \left(\frac{1}{\Delta t^2} \mathbf{m} \right) \mathbf{u}_{n-1} \quad (5)$$

from which we can solve for \mathbf{u}_{n+1} . As an explicit time integration method, the central difference method is conditionally stable and the time step size must be smaller than the critical time step.

\mathbf{f}_n is external force at the time of t_n . For the present problem, contact force between the tapping object

and the test structure is the only external force. The contact force \mathbf{f}_n is calculated by using dynamic contact algorithm based on the exterior penalty method. Contact condition is that the contacting bodies should not penetrate each other. However, in applying the exterior penalty method, small penetration is permitted and contact force is calculated by the penetration multiplied by given penalty parameter.

4. Calculation of tapping sound

Governing equation of the sound field radiated from vibrating surface can be analyzed using following Helmholtz equation and boundary conditions [8].

$$\nabla^2 p + k^2 p = 0 \quad \text{in } \Omega(x) \quad (6)$$

where, $k = \omega/c$ is wave number and boundary conditions are that ;

$$\frac{\partial p}{\partial n_s} = -\rho_0 \dot{y}_n \quad \text{on } \partial\Omega(x) \quad (7)$$

Both finite element method (FEM) and boundary element method (BEM) can be used to solve eq. (6). But BEM is more powerful than FEM in some problems like calculations of sound field, because BEM can solve boundary value problem only with meshes on the boundary and can treat infinite domain easily. So in this study, BEM is used for the calculation of radiated sound field.

To use BEM, following fundamental solution is introduced.

$$\nabla^2 p^* + k^2 p^* = \delta(x - x_s) \quad (8)$$

$$p^*(x, x_s) = -\frac{\exp(-jk|x - x_s|)}{4\pi|x - x_s|} \quad (9)$$

then, we can derive following integral equation.

$$\int_{\Omega} (p \nabla_s^2 p^* - p^* \nabla_s^2 p) dV = - \int_{\partial\Omega} \left[p \frac{\partial p^*}{\partial n_s} - p^* \frac{\partial p}{\partial n_s} \right] dS \quad (10)$$

and then,

$$\alpha p(x) = \int_{\partial\Omega} \left[p^* \frac{\partial p}{\partial n_s} - p \frac{\partial p^*}{\partial n_s} \right] dS(x_s) \quad (11)$$

where,

$$\alpha = \int_{\Omega} p \delta(x - x_s) dV \quad (12)$$

$$\alpha = \begin{cases} 1 & x \in \Omega \\ 1/2 & x \in \partial\Omega \\ 0 & \text{otherwise} \end{cases} \quad (13)$$

Using BEM, we can set a matrix equation on the surface $\partial\Omega$ as follows:

$$[A]\{P\}=[B]\left\{\frac{\partial P}{\partial n}\right\} \quad (14)$$

and

$$\left\{\frac{\partial P}{\partial n}\right\}=-\rho j\omega\{V_n\}=\rho\omega^2\{U_n\} \quad (15)$$

where, $\{V_n\}$ and $\{U_n\}$ are the normal velocity and displacement of fluid on the surface of structure in frequency domain, respectively.

Finally,

$$[A]\{P\}=[C]\{U_n\} \quad (16)$$

Now, we can calculate sound pressure in frequency domain with known values of $\{U_n\}$.

After calculating $\{P\}$ on the surface, pressure in the domain Ω can be obtained by equation (11). In this case, equation (11) is solved in the domain Ω using BEM.

$$P=\{A\}^T\{P\}+\{C\}^T\{U_n\} \quad (17)$$

The sound pressure data in time domain is calculated using the sound pressure data in frequency domain. If the sound pressure in time domain is calculated through FFT only with the sound pressure data in frequency domain, too many calculations are needed for enough number of data and several problems can occur, because of fixed Δt .

$$p(t)=\sum_{i=0}^{\infty}p_i e^{j\omega_i t}\cong\sum_{n=0}^{l-1}P(n)e^{j\omega(n)t} \quad (18)$$

where, $p(n)$ is (n-1)'th calculated pressure value, $\omega(n)$ is (n-1)'th angular velocity of calculated value, and l is total number of calculated frequency.

Here, an assumption introduced in equation (18) is adopted. In some cases, this assumption will produce wrong values because of improper selection of $\omega(n)$ as errors occur because of improper Δt in calculation of values in time domain. So $\omega(n)$ must be selected with care.

5. Feature Extraction from Tapping Sound

Unfortunately, it is very difficult to find a closed form relationship between the existence of defects and the tapping sound. To determine the existence of defects by comparing the tapping sound, we need a method that pictures the characteristics of the tapping sounds of an original healthy structure and a test structure. Therefore, feature data, which reflect the characteristics of tapping sound data, should be extracted from the raw tapping sound data. The well-extracted feature data is small number of data, which reflects the key feature of tapping sound data. After feature extraction, the feature data of sound print (tapping sound of

original healthy structure) and that of the tapping sound of test structure are compared to find the changes in the tapping sound due to the existence of subsurface defects.

Wavelet packet transform [9] was used as the feature extraction scheme. Wavelet packet transform is similar to the discrete wavelet transform except that the detail part is also decomposed to the sub level. The top level of a wavelet packet transform represents the original signal in respect to time. As the decomposition proceeds to sub levels, the frequency resolution increases. Wavelet packet transform of i -th level has 2^i packets.

After wavelet packet transform, the energy of each packet is used in a feature array [10]. The packet energy is defined as:

$$E_j^i = \sum_k^J P_{jk}^i \quad (19)$$

where, E_j^i is the packet energy of the j -th packet in the i -th level, P_{jk}^i is the wavelet packet coefficient of the j -th packet in the i -th level and J is the number of coefficient for that packet. After obtaining the feature array, the feature array of the healthy structures are set as the sound print of the structure and compared with the feature array of tapping sound from the real test structure.

6. Procedures of Making Sound Print

For each tapping point, one set of tapping sound simulation consists of following procedures:

- (1) Finite element calculation of the time history of nodal displacement due to tapping force.
- (2) Fourier transform of the time domain nodal displacement.
- (3) Boundary element calculation of tapping sound in frequency domain using the transformed displacement data.
- (4) Calculation of tapping sound in time domain by inverse Fourier transform.
- (5) Perform wavelet packet transform of tapping sound data
- (6) Calculation of feature array

Making sound print database requires many sets of tapping sound simulation with respect to each tapping point. If the test structure is large or the shape of test structure is complicated, many sets of tapping sound simulation should be needed. Each set of tapping sound simulation is independent and there is no coupling among each sets of tapping sound simulation. Therefore, each set of tapping sound simulation can be performed independently.

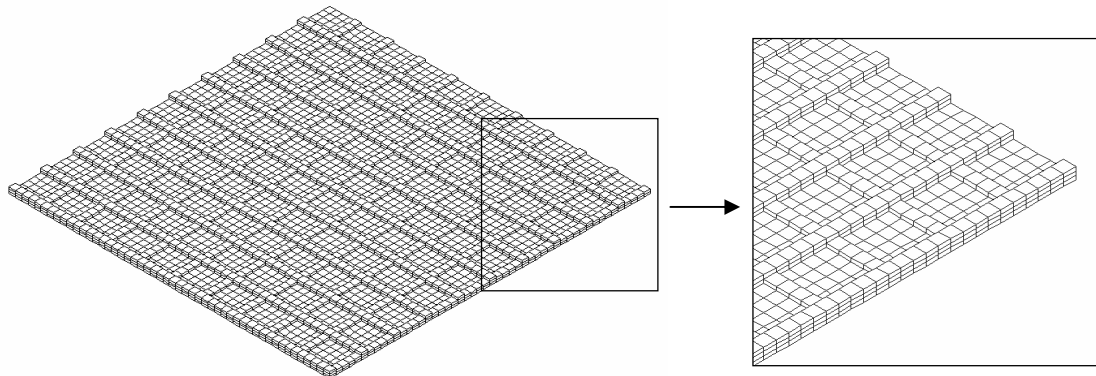


Figure 1: Finite element mesh of test structure

7. Making Sound Print Database of a Test Structure

As a demonstration of a sound print calculation, a $500 \times 500 \times 1$ mm composite plate (USN125BX) with reinforcement was chosen as a test structure. The thickness of reinforcement was 1 mm or 2 mm. Figure 1 shows the test structure of present work. Eight-node brick elements were used for the finite element mesh. Total finite elements were 3900 and total nodes are 7943. Total degree of freedom is 23,829. 900 tapping points were chosen for the calculation of sound print. Therefore, 900 times of tapping sound simulation were performed. The locations of 900 tapping points are depicted in Figure 2. Note that the test surface was the bottom of the test structure depicted in Figure 1 and the test surface was a flat surface. The tapping object was assumed as a rigid ball of 1 cm diameter. Mass of tapping object was 10 g and the tapping velocity was 0.1

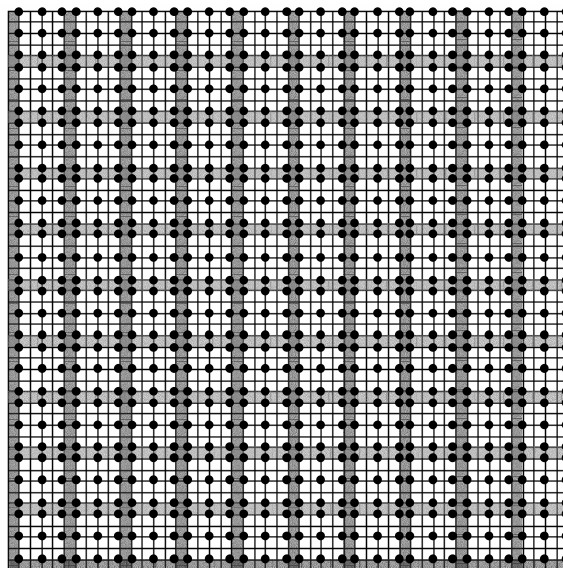


Figure 2: Tapping points for sound print database

m/sec. The time step for time integration was 1×10^{-7} sec and the terminal time was 1×10^{-2} sec. The boundary element mesh was the same as used for the finite element analysis. Four-node quadrilateral elements were used and the total number of boundary elements was $50 \times 50 = 2500$. Because the audible frequency range is 20Hz~20kHz and the sampling frequency was set to be 40 kHz. The sampling time was $1/40000 = 2.5 \times 10^{-5}$ sec. The tapping sound data was sampled at 10 cm above the tapping point. As a feature extraction method, 12-th order Daubechies' wavelet was used and 8-level wavelet packet transform was performed. Therefore, the number of components of feature array was $2^8 = 256$.

8. Departmental Computing GRID System

To solve the tapping sound simulations fast, DCG system composed of 122 PCs was utilized. The detail information about each PC in DCG was given in Table 1. As described in Table 1, three cluster systems (SSC1, SSC2 and SSC3 cluster system) and distributed PC-farm systems comprise DCG system. SSC1 cluster system has total 32 nodes and each node has dual Pentium III 1GHz processors with 1GB SDRAM memory, a 20 GB hard disk. In case of SSC2 cluster system, each node has dual Pentium III 550 MHz processors with 1 GB SDRAM memory, a 20GB hard disk. 16 nodes in SSC2 cluster system were available. Each node in SSC3 cluster system runs Intel Pentium IV 1.5 GHz processor on an Intel 850 chipset motherboard with 1 GB RDRAM memory, a 20 GB hard disk. SSC3 cluster system has 16 nodes. And 48 PCs (PC-farm system) distributed in several places were also used. Therefore, a total of 170 CPUs was used for tapping sound simulations as described in this session. In case of the PC-farm system, the configuration of PC is not homogeneous. There are various kinds of PC including Xeon system, Pentium III system, Pentium IV system,

Table 1: Departmental Computing GRID System

System	CPU	RAM	HDD	Number of CPUs
SSC1 Cluster	Pentium III 1 GHz (Dual)	SDRAM 1,024MB	20 GB	64(=32×2)
SSC2 Cluster	Pentium III 550 MHz (Dual)	SDRAM 1,024MB	20 GB	32(=16×2)
SSC3 Cluster	Pentium IV 1.5 GHz	RDRAM 1,024MB	40 GB	16(=16×1)
Distributed PC farm	Xeon 2 GHz (Dual)	RDRAM 2,048 MB	18 GB	2
	Pentium IV 2 GHz	RDRAM 1,024MB	60 GB	1
	Pentium IV 1.5 GHz	"	40 GB	2(=2×1)
	Pentium IV 1.4 GHz	"	"	1
	Pentium III 1 GHz (Dual)	SDRAM 1,024 MB	"	10(=5×2)
	Pentium III 866 MHz (Dual)	"	"	30(=15×2)
	Pentium III 650 MHz (Dual)	"	30 GB	2
	Athlon MP 1800+ (Dual)	DDR 1,024 MB	40 GB	2
	Athlon 1.33 GHz	SDRAM 1,024 MB	"	1
	Athlon 1 GHz	"	"	1
	Athlon 550 MHz	"	20 GB	6(=6×1)
Sum				170

Table 2 : CONDOR configuration

Master node configuration (SSC2 system)	Slave node configuration (SSC2 system)
MyType = "Machine"	MyType = "Machine"
TargetType = "Job"	TargetType = "Job"
Name = "ssc2.snu.ac.kr"	Name = "vm2@ssc201"
Machine = "ssc2.snu.ac.kr"	Machine = "ssc201"
Rank = 0.000000	Rank = Scheduler =?= "DedicatedScheduler@ssc2.snu.ac.kr"
...	...
DedicatedScheduler = "DedicatedScheduler@ssc2.snu.ac.kr"	DedicatedScheduler = "DedicatedScheduler@ssc2.snu.ac.kr"
CONDORVersion = "\$CONDORVersion: 6.3.1 Oct 8 2001 \$"	CONDORVersion = "\$CONDORVersion: 6.3.1 Oct 8 2001 \$"
CONDORPlatform = "\$CONDORPlatform: INTEL-LINUX-GLIBC22 \$"	CONDORPlatform = "\$CONDORPlatform: INTEL-LINUX-GLIBC22 \$"
...	...
UidDomain = "ssc2.snu.ac.kr"	UidDomain = "ssc201"
FileSystemDomain = "ssc2.snu.ac.kr"	FileSystemDomain = "ssc201"
Subnet = "192.168.0"	Subnet = "192.168.0"
...	...
TotalVirtualMachines = 1	TotalVirtualMachines = 2
...	...
Start = TRUE	Start = TRUE
Requirements = START	Requirements = START
CurrentRank = 0.000000	CurrentRank = 0.000000
...	...

Athlon system etc. The PCs of PC-farm system have been utilized as computing server, web server, and testbed system for numerical experiments and have been maintained by each laboratory of aerospace engineering department.

All of the PCs in DCG system are connected by a local area network (Fast Ethernet) and three cluster systems have an inner local network (ex. 192.168.*.*) with switching hubs. Master nodes in three cluster systems have two network interface cards for inner network and external network. Linux operating system was installed to each PC and MPICH-G2[11], LAM-MPI[12] were installed for parallel computing tests. Globus[3] (Ver. 1.1.4) was installed for constructing GRID system and CONDOR[5] (Ver. 6.3.1) was also installed for job-scheduling and submitting. CONDOR service was registered at *Globus jobmanager services* and the CONDOR policy for starting jobs was set as dedicated resources. Job submitting and monitoring can be executed at only master node in which CONDOR central manager was installed and job scheduling was also performed in master node. The detail configuration of master node and slave in CONDOR pool is given in Table 2. In CONDOR pool, file I/O operations were carried out through remote system call function built in CONDOR since any NFS system was not used. One CPU of master node was dedicated for CONDOR job running since the master node should do many operations for managing CONDOR jobs.

9. Load Balancing

A total of 900 jobs was performed through DCG system. Execution of 900 tapping sound simulations on DCG system involves distributing workload among the DCG system at runtime. Various load balancing schemes were suggested by several researchers [13, 14, 15]. In this work, a total of 900 jobs was divided into four subgroups considering the heterogeneous system performance before job running and four subgroups were allocated into three cluster systems and PC-farm system. And then, each job was launched and

Table 3: The benchmark results of PC-farm system

System	Node number	Benchmark results (minutes)	Equivalent weight	Total equivalent weight
Xeon 2 GHz (Dual)	2	38	4	8
Pentium IV 2 GHz	1	40	4	4
Pentium IV 1.5 GHz	2	53	3	6
Pentium IV 1.4 GHz	1	57	3	3
P III 1 GHz (Dual)	10	141	1	10
P III 866 GHz (Dual)	30	162	1	30
P III 650 MHz (Dual)	2	215	0.5	1
Athlon MP 1800+ (Dual)	2	56	3	6
Athlon 1.33 GHz	1	85	2	2
Athlon 1 GHz	1	121	1	1
Athlon 550 MHz	6	132	1	6
Sum				77

monitored through CONDOR. The size of input and output file was less than 0.6 MB and the temporary files was written and read in local hard disk memory. Therefore, the network overloading for input file distribution and output file collection carried out by CONDOR was not a serious problem. So, the dynamic network load was not considered for load balancing in this work

To take into the heterogeneity of system performance, a widely used mechanism is to assign a relative weight measuring the relative performance to each processor. In case of DCG system, PC-farm system has a complex heterogeneity of processors. The system performance of three clusters is also different even though each cluster system has a homogeneous system configuration. Therefore, a benchmark test must be needed to measure the relative performance of four systems in DCG system. For performance benchmark, one test problem selected randomly among 900 tapping sound simulations, which have all the same floating-operation counts, was executed in each system. In case of PC-farm system, total 11 PCs were chosen for the benchmark test because one system among the PCs, which have the same configuration, was selected. Two jobs were run simultaneously in case of dual system to consider the system performance deterioration due to sharing system resources by two jobs. The maximum elapsed time among 10 runs was selected as the benchmark result. The elapsed time of SSC1 system, SSC2 system and SSC3 system was 144 min., 230 min. and 44 min. respectively. The benchmark results of PC-farm system are given in Table 3. In Pentium III 866 MHz dual system, the required elapsed time was 162 min and this period was defined as a unit period. And then, the equivalent weight was calculated based on these benchmark results. The equivalent weight means the job number that can be executed within the unit period. The total calculated equivalent weight of PC-farm system was 77 as shown in Table 3. In other words, the computing performance of PC-farm system may be considered to be equivalent as that of a cluster system that has 77 Pentium III 866 MHz processors. This equivalent system model of PC-farm was utilized for load balancing. To find a best load balancing result, a simple optimization problem was introduced as follows:

Minimize $Max (f_1(\alpha), f_2(\beta), f_3(\gamma), f_4(\eta))$

Constraints: $64\alpha + 32\beta + 16\gamma + 77\eta = 900$ ($\alpha, \beta, \gamma, \eta$: Integer number)

$1 \leq \alpha \leq [900/64]^*$, $1 \leq \beta \leq [900/32]$, $1 \leq \gamma \leq [900/16]$, $1 \leq \eta \leq [900/77]$

where $f_1(\alpha) = 141\alpha$, $f_2(\beta) = 230\beta$, $f_3(\gamma) = 44\gamma$, $f_4(\eta) = 162\eta$

$\alpha, \beta, \gamma, \eta$: the number of jobs executed in each node of SSC1, SSC2, SSC3 and PC-farm system

After some calculations, the optimal value of α, β, γ and η was 4, 3, 15, and 4 respectively and the estimated total elapsed time was 690 minutes. This result means that the number of jobs allocated to SSC1, SSC2, SSC3 and PC-farm system was 256, 96, 240, and 308 respectively.

10. Numerical Result

900 cases of tapping sound simulation were performed using SSC System. Output data of program was time histories of contact force and tapping sound. Figure 3 shows the examples of contact force profile. The contact force profiles are different at different tapping point. At the region of large thickness, where contact stiffness is relatively high, contact duration is short and peak of contact force is high. And, at the region of small thickness, contact duration is long and peak of contact force is low. Figure 3 shows these contact characteristics. Though contact force profile possesses other useful information, contact duration was considered in this study. After calculation of contact profile, contact duration was measured. Figure 4 shows

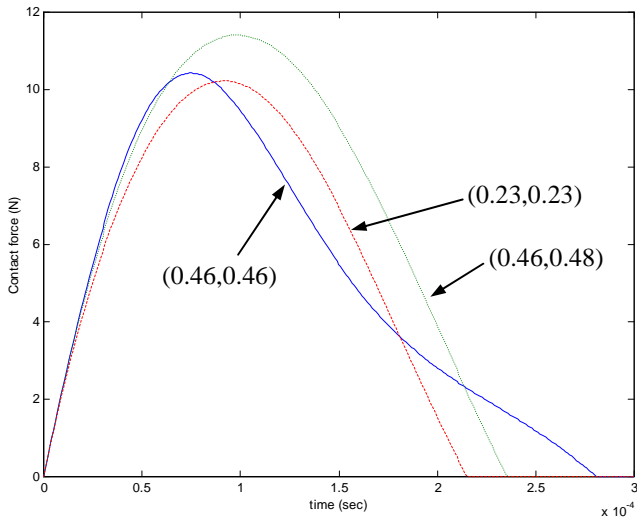


Figure 3: Contact force profile

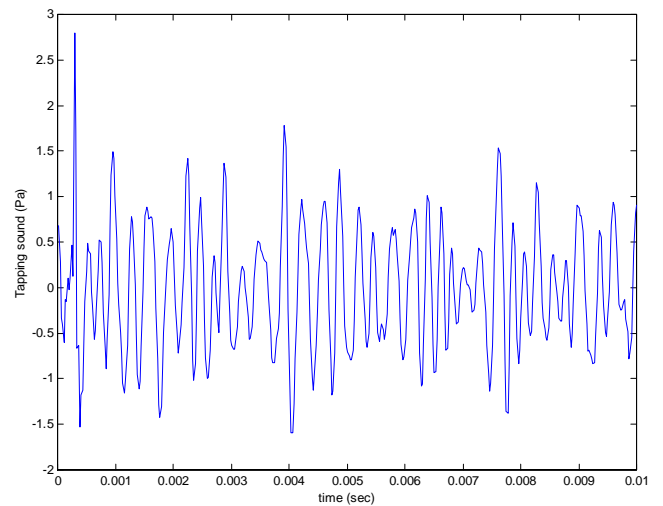


Figure 4: Time history of tapping sound

* $[x]$ = the minimum integer greater than x

the time history of tapping sound. As mentioned previously, direct comparison of tapping sound data is nearly impossible and inefficient. Therefore, the time data of tapping sound was converted to feature array by using wavelet packet transform according to the feature extraction method.

As a graphical presentation of subsurface condition of the present test structure, contour of contact

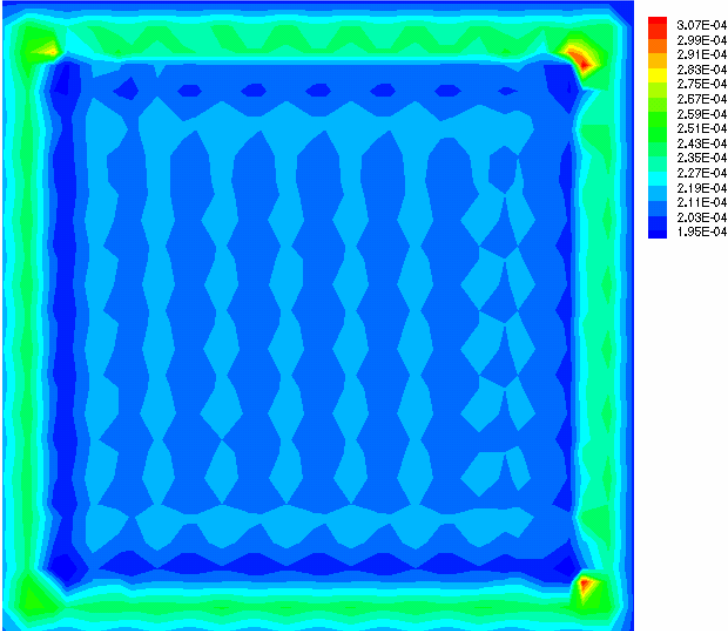


Figure 5: Contour of contact duration over a reinforced plate

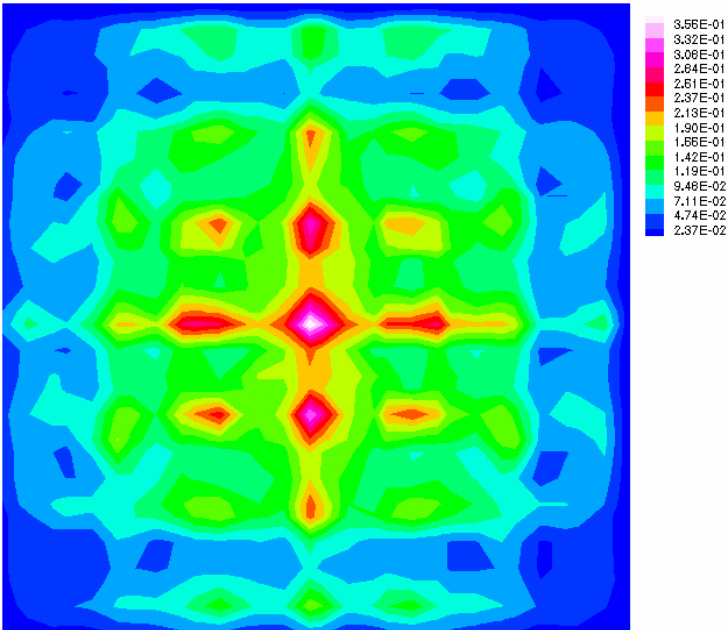


Figure 6: Contour of tapping sound over a reinforced plate

duration and tapping sound were plotted. Figure 5 shows the contour of contact duration of present test structure and Figure 6 shows the contour of tapping sound of present test structure. To show the tapping sound data as a single value, norm of feature array was taken as a single value to represent the tapping sound data. Figure 6 is sound print plot of present test structure.

Sound print database such as Figure 6 is obtained *a priori* and the real inspection process is measuring the tapping sound data of real test structure and converting the tapping sound data to feature data and comparing the sound print and real tapping sound data to determine the subsurface defects.

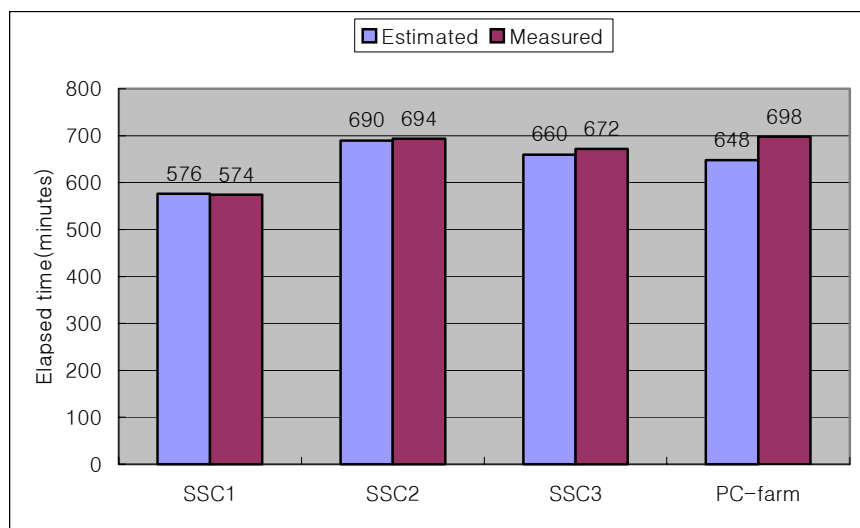


Figure 7: The elapsed time of each system

According to the load-balancing result, the estimated total elapsed time was 690 minutes. The measured total elapsed time was 698 minutes. However, the elapsed time of SSC2 system was expected to be the maximum value but the maximum elapse time was measured in PC-farm system as shown in Figure 7. The total elapsed time of SSC1 system, SSC2 and SSC3 system was almost exactly predicted since the real system performance can be measured by the benchmark test. In case of PC-farm system, there is a relatively large difference due to the error between the real system performance and the equivalent model system performance used in load balancing.

In Table 4, the number of jobs executed in each system (N_j) is tabulated. As expected before, the N_j of each cluster system was 256, 96 and 240 respectively. The N_j of PC farm system differed from 5 to 120. As shown in Figure 8, the number of jobs executed per CPU (N_c) was 4, 3 and 15 respectively in three cluster systems and the N_c of PC farm system differed from 3 to 17. The N_c of Xeon 2.2 GHz system was the maximum value and the N_c of PIII 550 MHz was the minimum value.

During single job execution, the required RAM and HDD memory was 404 MB and 120 MB respectively.

Therefore, total required RAM and HDD memory was 363.6 GB and 108 GB respectively. The floating-point operation count per single job² was about 178 Gflops and the total number of floating-point operations performed during NDE simulations was 160 Tflops. Therefore, the sustained performance during NDE simulations was 3.84 Gflops/sec. If 900 jobs were executed on single machine, it would take about 12 days even though the most powerful Xeon 2 GHz system was dedicated to the jobs. This means that it is impractical to use tapping sound analysis for determining existence of defects inside the structure without Grid computing technology.

Table 4 : The number of jobs executed in each system (N_j)

System	CPU	Number of CPUs	N_j (Number of Jobs)
SSC1 Cluster	Pentium III 1 GHz (Dual)	64	256
SSC2 Cluster	Pentium III 550 MHz (Dual)	32	96
SSC3 Cluster	Pentium IV 1.5 GHz	16	240
Distributed PC farm	Xeon 2 GHz (Dual)	2	34
	Pentium IV 2 GHz	1	15
	Pentium IV 1.5 GHz	2	24
	Pentium IV 1.4 GHz	1	11
	Pentium III 1 GHz (Dual)	10	40
	Pentium III 866 MHz (Dual)	30	120
	Pentium III 650 MHz (Dual)	2	6
	Athlon MP 1800+ (Dual)	2	22
	Athlon 1.33 GHz	1	7
	Athlon 1 GHz	1	5
	Athlon 550 MHz	6	24
Sum		170	900

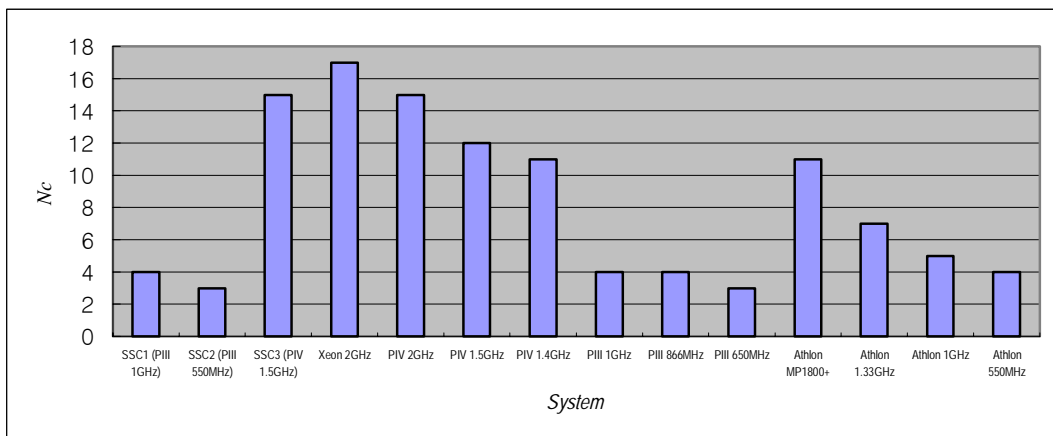


Figure 8: The number of jobs executed per CPU (N_c)

² The floating-point operation count was measured by *perfex* command in SGI Onyx2 system

11. Concluding Remarks

In this work, an application of Grid computing technology to a solution of real engineering problem was presented. We utilized the Grid computing technology to the development of a new non-destructive evaluation method, which utilizes the tapping sound data to find the subsurface defects. This new NDE method as an artificial intelligent tapping inspection method is named Tapping Sound Analysis. The inspection process is comparing real measured tapping sound data and pre-obtained reference tapping sound data, which is defined sound print. The key feature of Tapping Sound Analysis is that the reference data of inspection is obtained by using high precision numerical simulation. For the objectivity and absoluteness of sound print, the tapping sound generation mechanism was numerically modeled. In order to obtain sound print database, many times of tapping sound simulation are required. Therefore, Grid computing technique was utilized in the sound print database calculation. A total of 900 tapping sound simulation jobs was executed by DCG system composed of 122 distributed PCs and it took about 11 hrs to run all jobs. The computing resources of distributed PCs were successfully utilized through *Globus* and *CONDOR* without any additional investment. This means that the Grid computing technology reduces the necessary time for Tapping Sound Analysis and makes TSA a feasible and practical methodology.

ACKNOWLEDGEMENT

The research was supported by a grant from the Ministry of Science and Technology through the National Research Laboratory Programs (Contract number 00-N-NL-01-C-026).

References

1. Kim, S.J. and Hwang, J.S., "New Nondestructive Evaluation Method of Laminated Composite Structures by Tapping Sound Analysis", *SPIE's 6th Annual International Symposium on NDE for Health Monitoring and Diagnostics*, Newport Beach, California, U.S.A, March, 2001
2. I. Foster and C. Kesselman, *The Grid: Blueprint for a New Computing Infrastructure*, Morgan Kaufmann Publishers, San Francisco, California, 1999
3. Globus Project Team, *Globus Project*, World Wide Web, <http://www.globus.org>
4. A. Grimshaw and W. Wulf, The Legion Vision of a Worldwide Virtual Computer, In *Communications of the ACM*, 40(1), January, 1997
5. CONDOR Team, *CONDOR High Throughput Computing*, World Wide Web, <http://www.cs.wisc.edu/condor>
6. Goo, N.S., and Kim, S.J., "Dynamic Contact Analysis of Laminated Composite Plates Under Low-Velocity Impact", *AIAA Journal*, Vol.35, No.9, Sept, 1997, pp.1518-1521
7. K. J. Bathe, *Finite Element Procedures in Engineering Analysis*, Prentice Hall Inc., Englewood Cliffs, New Jersey, 1982
8. H. Kane, James, *Boundary Element Analysis in Engineering Continuum Mechanics*, Prentice Hall Inc., Englewood Cliffs, New Jersey, 1994
9. Coifman, R. and Wickerhauser, M., "Entropy-based algorithms for best basis selection," *IEEE Transaction on information theory*, Vol 38, No. 2, 1992, pp.713-718
10. Staszewski, W.J., "Wavelet based Compression and Feature Selection for Vibration Analysis," *Journal of Sound and Vibration*, Vol. 211, No. 5, 1998, pp. 735-760

11. MPICH Group, *MPICH-G2*, World Wide Web, [http:// www3.niu.edu/mpi/](http://www3.niu.edu/mpi/)
12. LAM Team, LAM/MPI Parallel Computing, World Wide Web, <http://www.lam-mpi.org>
13. L. Oliker and R. Biswas, "PLUM:Parallel Load Balancing for Adaptive Refined Meshes," *In Journal of Parallel and Distributed Computing*, 47(2):109-124,1997
14. M. Willebeek-LeMair and A. Reeves, "Strategies for Dynamic Load Balancing on highly Parallel Computers," *In IEEE Transactions on Parallel and Distributed Systems*, 4(9):979-993, September 1993
15. Z. Lan, V. E. Taylor, and G. Bryan, "Dynamic Load Balancing of SAMR Applications on Distributed Systems," SC2001, Denver, Colorado, November, 2001